

Carlo Martinoli  
Stefano Bianchi  
M'Hamed Dahmane  
Francesca Pugliese  
Maria Pia Bianchi-Zamorani  
Maura Valle

## Ultrasound of tendons and nerves

Published online: 19 October 2001  
© Springer-Verlag 2001

\* Categorical Course ECR 2002

C. Martinoli (✉) · M. Dahmane · F. Pugliese  
Cattedra di Radiologia "R" – DICMI –  
Università di Genova,  
Largo Rosanna Benzi 8,  
16132 Genova, Italy  
e-mail: martinoli@zeus.newnetworks.it  
Fax: +39-010-3537213

S. Bianchi  
Département de Radiologie,  
Division de Radiodiagnostic  
et de radiologie interventionnelle,  
Hôpital cantonal Universitaire de Genève,  
1211 Geneva, Switzerland

M.P. Bianchi-Zamorani  
Unité de Développement et de Recherche  
des Etudes Médicales (UDREM),  
Université de Genève, 1211 Geneva,  
Switzerland

M. Valle  
Istituto Scientifico "Giannina Gaslini",  
16128 Genova, Italy

**Abstract** Tendons and nerves represent probably one of the best application of musculoskeletal US due to the high lesion detection rate and accuracy of US combined with its low cost, wide availability, and ease of use. The refinement of high-frequency broadband linear-array transducers, and sensitive color and power Doppler technology, have improved the ability of US to detect fine textural abnormalities of these structures as well as to identify a variety of pathological conditions. Characteristic echotextural patterns, closely resembling the histological ones, are typically depicted in these structures using high US frequencies. In tendon imaging, US can assess dislocations, degenerative changes and tendon tears, including intrasubstance tears, longitudinal splits, partial and complete rupture, inflammatory conditions and tendon tumors, as well as postoperative

findings. In nerve imaging, US can support clinical and electrophysiological testing for detection of compressing lesions caused by nerve entrapment in a variety of osteofibrous tunnels of the limbs and extremities. Congenital anomalies, nerve tears, and neurogenic tumors can also be diagnosed. Overall, US is an effective technique for imaging tendons and nerves. In most cases, a focused US examination can be performed more rapidly and efficiently than MR imaging.

**Keywords** Tendons · Nerves · Musculoskeletal system · Peripheral nervous system · Ultrasound

### Introduction

With technologic advances achieved over the past few years, including refinement of high-frequency broadband transducers, introduction of extended field-of-view techniques and sensitive color and power Doppler imaging, the role of US as the first-line imaging modality in the assessment of disorders affecting tendons and nerves has been further strengthened and has gained full acceptance [1, 2, 3, 4]. When US is used as the initial investigation after clinical assessment, it may provide information that obviates the need for more costly imaging studies, such as MR imaging, in a relatively inexpensive and widely accessible way.

The objective of this article is to review the US appearance of normal tendons and nerves, and to describe the main US findings in the most common disorders affecting these structures.

### Normal ultrasound anatomy

Although tendons and nerves share some characteristics, such as dimensions, tubular conformation, and striated appearance, a careful analysis of their echotexture by means of high-frequency probes can provide the main differential criteria. In fact, the US appearance of both

normal tendons and nerves is fairly uniform and closely reflects their histologic composition [5]. Tendons have a fibrillar pattern of parallel hyperechoic lines in the longitudinal plane which are due to a series of specular reflections at the boundaries of collagen bundles and endotendineum septa and a hyperechoic round to ovoid image containing bright stippled clustered dots instead of the linear fibrillar echoes in the transverse plane (Fig. 1a, b) [6, 7]; nerves have a fascicular pattern made of multiple hypoechoic parallel linear areas separated by hyperechoic bands, in which the hypoechoic structures correspond to the neuronal fascicles that run longitudinally within the nerve, and the hyperechoic background relates to the interfascicular epineurium (Fig. 1c) [1, 8, 9]. On transverse scans, nerves assume a honeycomb-like appearance with hypoechoic rounded areas embedded in a hyperechoic background (Fig. 1d).

When arising from more than one muscle, tendons exhibit a laminated appearance made of separate groups of fibers that overlie or twist one another [10, 11]. Depending on the rectilinear or curved tendon path, different tissue envelopes invest the tendons to reduce the friction during movements and the likelihood of resulting injuries: the paratenon, a loose areolar and adipose tissue envelope, surrounds tendons with rectilinear course; the synovial sheath covers curvilinear tendons which pass through osteofibrous tunnels to redirect their course across synovial joints [5]. While the paratenon appears as a thin hyperechoic line surrounding the tendon boundaries, the synovial sheath can be appreciated with US only when a small effusion is comprised within the synovial space.

Different from tendons, nerves are compressible and change in shape depending on the volume of the anatomic spaces within which they proceed as well as on the bulk of the perineural structures. Usually, the nerves course very close to the vessels, even bulging into the vein occasionally. With even slight pressure applied with the US probe, they may be seen sliding to the side on the surface of an artery or a muscle. When nerves cross tight passages (i.e., neural foramina, osteofibrous tunnels), they may assume a more homogeneous hypoechoic appearance due to a tight package of the fascicles [12, 13, 14]. The overall number of fascicles in a nerve may vary depending on the occurrence of nerve subdivisions. In nerve bifurcations, the nerve trunk divides into two or more secondary nerve bundles, whereas each fascicle enters only one of the divisional branches without splitting. The outer boundaries of nerves are usually undefined due to a similar hyperechoic appearance of both the superficial epineurium and the surrounding fat.

Across the joints, both synovial sheath tendons and nerves pass through narrow anatomic passageways, the osteofibrous tunnels, that redirect their course. The floor of these tunnels consists of bone, whereas the roof is

made of focal thickenings of the fascia, the retinacula, that prevent dislocation and traumatic damage of the structures contained in the tunnel during joint activity. With high-frequency probes, retinacula can be seen at US as thin anisotropic laminar bands that overlie tendons and nerves [15]. Identification of an intervening hypoechoic space or dynamic scanning facilitate differentiation of fixed retinacula from gliding tendons.

---

### Ultrasound technique

Successful US examination of tendons and nerves can be carried out with almost any US machine equipped with linear high-frequency transducers ranging from 5 to 13 MHz frequency, being the optimal US frequency related with patient's body habitus and depth of the structure to be examined.

While scanning a tendon, the US beam should be oriented perpendicular to its longitudinal axis to better visualize its normal fibrillar pattern. Analysis of the fibrillar pattern may not be easy since even slight obliquity in transducer orientation can cause dramatic variation in tendon echogenicity, resulting in a hypoechoic appearance which may mimic tendon abnormalities (Fig. 2) [16]. This artifact derives from the strong anisotropic properties of tendon structure and is typically observed if a curved, rather than linear-array transducer, is used, or when tendons have curvilinear shape or oblique orientation to the skin surface, such as in the area of tendon attachment to bone. Depending on the anatomic site, a proper transducer position perpendicular to the tendon examined may be reached by either rocking the probe back and forth, pushing the probe obliquely against the patient's skin, or actively moving the joint examined while keeping the transducer fixed, or inducing tension in the examined tendon by active contraction of the muscle. Dynamics of tendon motion during joint movement or muscle contraction can be evaluated with US in real time, and this may be essential to rule out tendon pathology, to differentiate partial from complete ruptures, as well as to assess the status of a postoperative tendon.

Detection of nerves with US primarily depends on their size and course. Nerves are much less anisotropic than tendons and, therefore, do not require particular attention to maintain an adequate probe orientation during scanning [9]; however, systematic scanning on transverse planes is preferred to follow up the nerves contiguously throughout the limbs. For this purpose, longitudinal scans are less indicated because the nerve fascicles may be easily confused with echoes from muscles and tendons coursing along the same plane [17]. Color Doppler can aid in differentiating the hypoechoic nerves fascicles from adjacent hypoechoic small vessels.

**Fig. 1 a, b** Tendon and **c, d** nerve echotexture. **a** Long- and **b** short-axis 12- to 5-MHz US scan of Achilles tendon (*arrowheads*). In **a**, the fibrillar echotexture of the tendon is made of fine, parallel, and linear echoes. Paratenon appears as a hyperechoic envelope in continuity with subcutaneous fat. **c** Long- and **d** short-axis 12- to 5-MHz US scan of median nerve (*arrowheads*). In **c**, the fascicular echotexture of the nerve is composed of parallel linear hypoechoic areas separated by hyperechoic bands, an appearance quite different from that of tendon depicted in **a**. **d** On transverse scans, the nerve is characterized by a honeycombing appearance made of rounded hypoechoic areas in a hyperechoic background

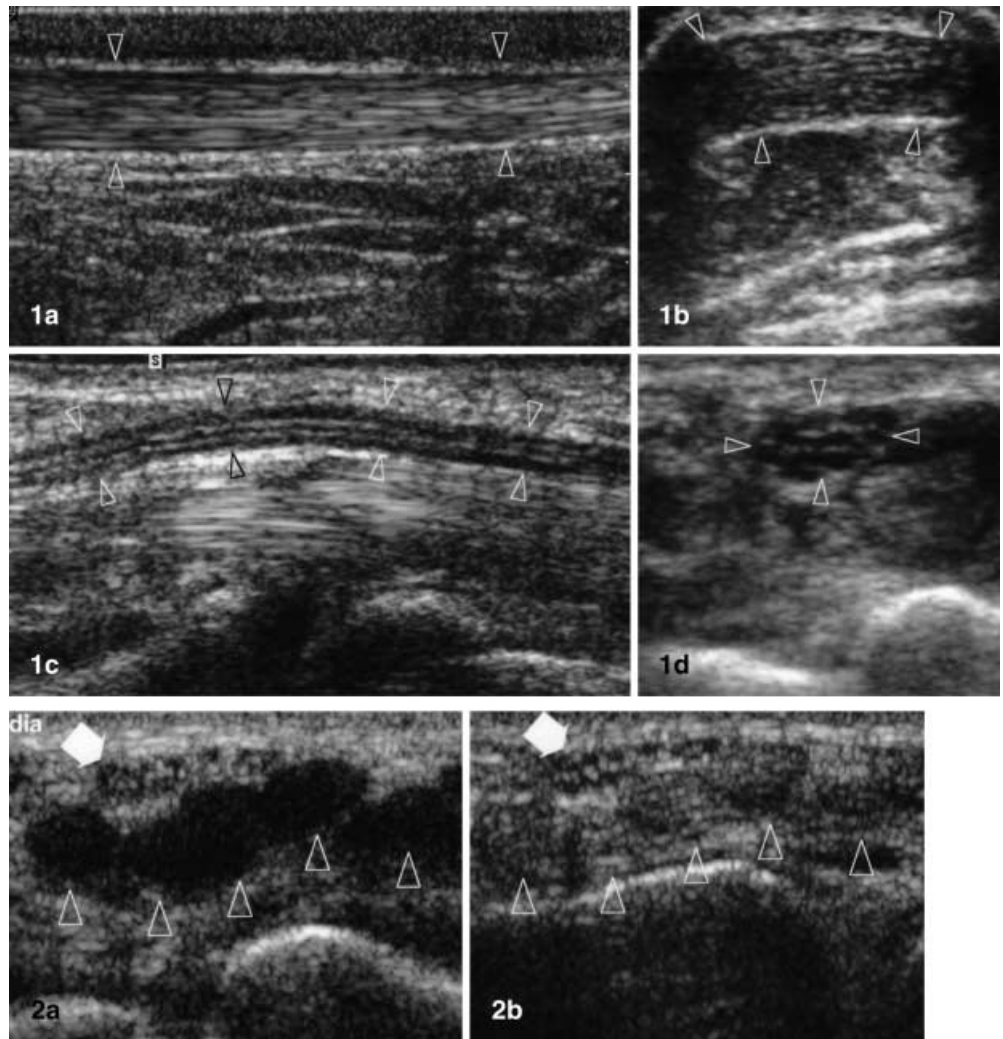


**Fig. 2a, b** Tendon anisotropy. Transverse 12- to 5-MHz US images of the flexor tendons at wrist obtained with an angle of incidence of the US beam **a** other than or **b** equal to  $90^\circ$ . **a** An artificial hypoechoic appearance is obtained when tendons (*arrowheads*) are imaged with the US beam at an inappropriate angle. This is in contrast to the normal hyperechoic fibrillar appearance displayed when the US beam is perpendicular to the tendon axis (**b**). Note that the fascicular structure of the median nerve (*arrow*) is always apparent regardless of angle of incidence, since nerves do not feel anisotropy

## Pathologic changes

A wide spectrum of tendon and nerve lesions are encountered in clinical practice, including degenerative conditions and traumas, entrapment, or dislocation – that typically occur at the osteofibrous tunnels – inflammatory and infectious diseases, and space-occupying lesions.

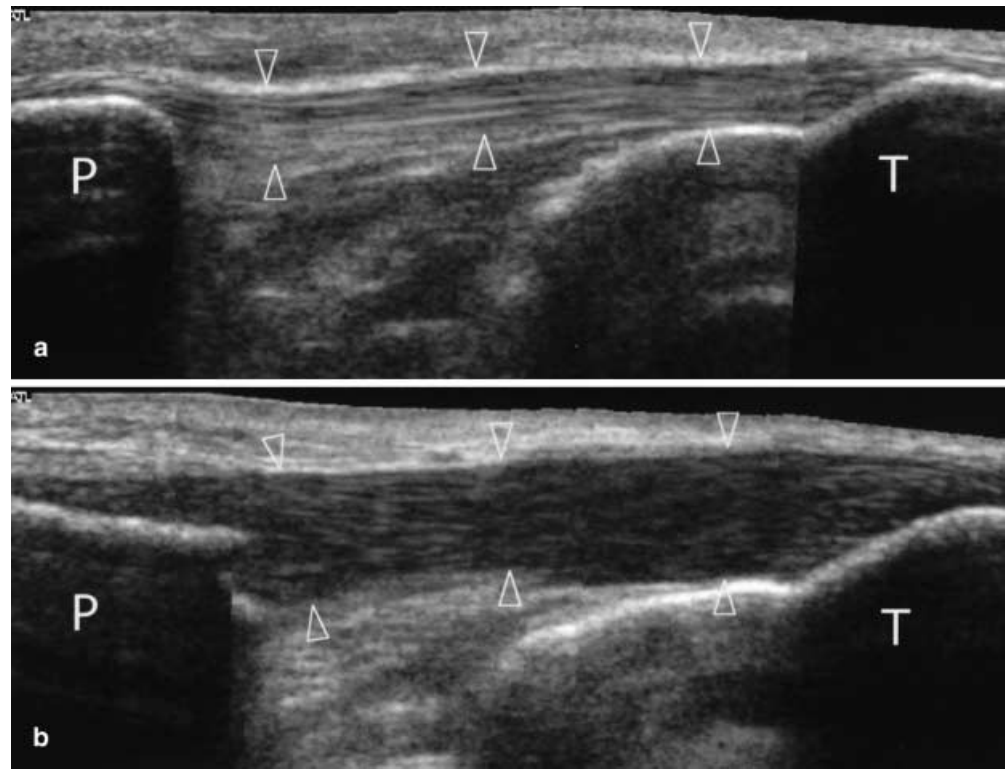
### Degenerative conditions and traumas

Tendon ruptures rarely occur outside the setting of predisposing degenerative changes that weaken the strength of tendinous structure. Numerous theories attempt to explain the degenerative process in tendons. Intrastance degeneration may derive from overuse injuries, such as occur in certain activities in which repetitive submaximal loading and/or eccentric mechanical forces create

microdamages that do not heal completely, especially in the vulnerable areas where tendons exhibit reduced blood flow [18]; however, constriction behind a retinaculum as well as excessive frictional forces against bony surfaces or adjacent accessory tendons can also contribute to tendon damage. In addition, abuse of corticosteroids and systemic disorders (i.e., rheumatoid arthritis, systemic lupus erythematosus, gout) can lead to tendon rupture. The quadriceps and patellar tendons, the extensor and flexor digitorum tendons, and the posterior tibial tendon are primarily affected by these settings. Most likely, some combination of trauma and predisposing factors, either mechanical or biochemical, is the initial cause of tendon degeneration. Then, a disease progression exists with tendinosis and minor intrastance tear leading to a partial or complete rupture.

The usefulness of US examination relies on how accurately this technique can distinguish a tendon tear from other pathologic conditions (i.e., tenosynovitis).

**Fig. 3a, b** Tendinosis. Longitudinal 12- to 5-MHz extended field-of-view US image of the patellar tendon (*arrowheads*) in **a** normal subject and **b** in patient with diffuse patellar tendinosis. In **b**, the abnormal tendon is diffusely thickened and shows heterogeneous hypoechoic echotexture. *P* patella; *T* tibia



Complete tendon tears do not usually give diagnostic difficulties, and a US study is rarely needed because the diagnosis is clinically obvious; however, tendon ruptures may be overlooked at certain sites or when severe pain limits the physical examination. In these settings, the role of US is critical in avoiding a delayed diagnosis because tendons retract with time, making retrieval and reattachment more complicated. A US evaluation may help in assessing the severity and extent of tendon injury. Information regarding the size of the gap between the tendon ends or the state of the torn tendon fibers in complete rupture can aid the surgeon in selecting the best operative approach. In partial tears the clinical diagnosis is more challenging and US can be helpful in distinguishing a tendon tear from other disease processes. An early US identification of subtle tendon abnormalities has a definite influence on the clinical outcome, because these signs allow establishment of conservative measures before the stage of rupture is reached.

Degenerative changes, also referred to as tendinosis, are associated with tendon swelling, tenderness, and absent or moderate pain aggravated by activities and coexistence of tenosynovitis. Focal or diffuse textural heterogeneity with hypoechoic areas, intratendinous hyperemia, and calcifications are the main US findings (Fig. 3) [2, 7, 19]. Histopathologic correlation has demonstrated that the abnormal tendon echotexture is secondary to fibromixoid degeneration and repair rather than inflammation [20, 21]. The degenerative process may selectively

be located either at the insertions (i.e., jumper's knee, lateral epicondylitis) or within the midsubstance (i.e., Achilles tendon) of tendons [22, 23, 24, 25]. The Achilles tendon is most commonly involved by metabolic disorders: in gout, urate tophi deposition may result in diffuse thickening of the tendon or intratendinous nodules; in familiar hypercholesterolemia, US recognizes intratendinous xanthomas as focal or diffuse hypoechoic areas before they become apparent clinically [26, 27, 28, 29]. Calcifications may seldom be encountered in the tendon substance, although their relation to tendon degeneration is unclear [30]. Calcific deposits may appear as linear echoes located at the insertion of tendon into bone, reflecting a process of calcium hydroxyapatite or calcium pyrophosphate dihydrate crystal deposition [31, 32]. In children, calcifications at the bony attachment of patellar tendon to the inferior pole of the patella (Sinding-Larsen-Johansson disease) and the tibial apophysis (Osgood-Schlatter disease), focal hypoechoic swelling of the physeal cartilage, and irregularities in the bony outlines are related to osteochondrosis, and may represent the end result of avulsion injuries confined to the unossified skeleton [33, 34].

Partial tears occur either in the transverse orientation or in the longitudinal direction parallel to the tendon fibers (longitudinal splits, fissurations). In transverse tears, US shows both the intact and the retracted ruptured portions of tendon in association with a hypoechoic blood collection [35, 36, 37]. Lack of tendon retraction is the

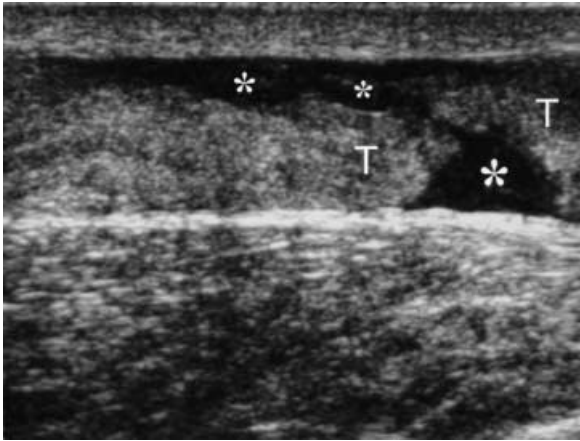


**Fig. 4** Complete tendon tear. Longitudinal 10- to 5-MHz US scan at the posterior ankle shows a transverse hypoechoic gap filled with echogenic blood effusion (*asterisks*) between the proximal and distal ends (*T*) of the Achilles tendon, consistent with a complete rupture

most important feature in distinguishing partial from complete rupture. Also, a localized irregularity of the tendon surface may be a useful finding in recognizing partial tears [2, 37, 38]. Longitudinal intrasubstance tears are demonstrated as a hypoechoic cleft within the tendon that may or may not reach the tendon surface. This kind of tear typically occurs at the level of ankle tendons [39, 40].

The acute complete rupture of a tendon appears as a focal gap created by a variable retraction of the torn edges of the tendon (Fig. 4) [6, 7, 38, 41]. The defect usually fills in with a hypoechoic blood collection. When the tendon sheath is also ruptured, the hematoma is usually larger and has irregular and indistinct margins. In subacute and chronic tearing, the absence of fresh hemorrhagic fluid and the organized hematoma which fills in the defect with echogenic material can be misleading, mimicking tendon integrity. In synovial sheath tendons, an accurate scanning technique may be required to visualize the tendon ends, which can be retracted from the site of the tear, as well as to measure the amount of tendon retraction on longitudinal scans [39, 42, 43, 44, 45]. If there is no retraction and the torn tendon ends are curled up, or if fluid does not fill the space created by the tear, passive assisted movements can be helpful by enhancing the separation of the tendon ends during stretching [10]. Intense muscle contraction or abnormal stress forces exerted on healthy tendons may lead to avulsions at their sites of insertion into bone. The size and degree of displacement of the avulsed bony fragment is variable depending on the affected tendon.

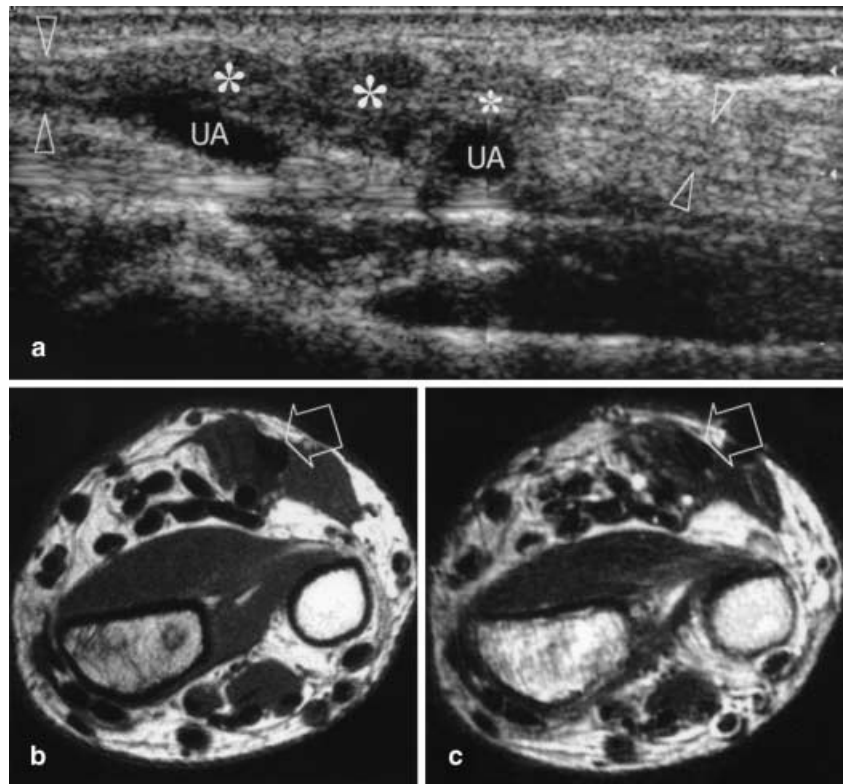
The mechanism of nerve damage in traumas does not depend on predisposing degenerative changes, but it de-

rives from either nerve stretching, which often occurs in association with a twist or sprain, or direct nerve contusion or laceration (i.e., penetrating wound). In certain subjects overuse can also lead to microtraumas related with abnormal tension or compression of the nerve. In mild injuries, the nerve may retain a normal US appearance regardless of clinical symptoms and functional deficit. Clinically, the absence of textural abnormalities seems to correlate with a higher probability of functional recovery. When the trauma is more significant, focal hypoechoic changes with loss of the fascicular pattern and increased local blood flow are seen in association with a hematoma [8, 46, 47]. Then, a fusiform local swelling of the nerve, commonly referred to as traumatic neuroma, develops as a result of the reparative process and fibrosis [1, 48]. This can be appreciated as an elongated hypoechoic mass at the site of the injury, characterized by irregular or poorly defined borders by adhesions, that rapidly grows after the trauma (Fig. 5). If there is complete nerve transection and a too wide gap keeps the nerve ends separated one another, the neuroma usually arises from the proximal nerve edge [46]. Traction injuries may cause the avulsion of nerve roots at the level of neural foramina. These lesions typically involve the brachial plexus and cause either swelling or disruption of the nerve continuity with retraction and wavy course of the distal nerve end. An extradural anechoic collection of cerebrospinal fluid, the pseudomeningocele, may be observed outside the neural foramina.

#### Disorders related to osteofibrous tunnels

At the osteofibrous tunnels, the absence of retinacula that retain down either tendons invested by synovial sheath or nerves may lead to instability of these structures with subluxation and dislocation from their groove. Dynamic US scanning is well suited for such evaluation, especially in cases of subluxation, where this technique is more efficient and easier than MR imaging obtained with varied positioning [49]. Permanent dislocations may readily be identified on static scans, whereas intermittent subluxation requires dynamic examination to assess whether reduction may be spontaneous or not. A spectrum of mechanical injuries to the retinacula may lead to tendon instability. Ultrasound may reveal the tendon displacement as well as numerous associated findings, such as peritendinous effusion related to tenosynovitis or lesions in the tendon substance due to abnormal friction against bony edges. Transverse planes perform better to assess the dislocation of tendons, because both the empty tunnel and the displaced tendon can usually be seen in a single image. The tendons that are more susceptible to dislocation are the long head of biceps tendon [49, 50, 51], the peroneal tendons [52, 53], and the flexor digitorum tendons [15, 54, 55, 56].

**Fig. 5a–c** Nerve trauma. **a** Longitudinal 12- to 5-MHz US scan with **b** T1-weighted spin-echo (SE) and **c** T2-weighted turbo SE MR imaging correlation shows a traumatic neuroma (*asterisks*) within the substance of the ulnar nerve at the distal forearm of a patient with partial transection of the nerve by a penetrating wound. The neuroma develops from the resected fascicles of the ulnar nerve (*arrowheads*) as a fusiform hypoechoic and irregular mass. On correlative transverse MR images, the neuroma (*arrow*) shows low intensity signal due to its fibrotic nature



Similar to tendons, nerves may dislocate too. This typically occurs at the elbow, where the ulnar nerve lies in an osteofibrous ring, the cubital tunnel, formed by a groove between the olecranon process and the medial epicondyle and bridged by the Osborn retinaculum. If the retinaculum is loose or absent, dynamic examination during elbow flexion can depict the intermittent dislocation of the ulnar nerve over the epicondyle [57]. Dislocation of the medial edge of the triceps can also occur in combination with dislocation of the ulnar nerve.

Generally, this condition is asymptomatic and may be associated with snapping sensation and discomfort while the flexed elbow touches the table; however, the repeated friction of the nerve against the epicondyle can cause chronic damage and functional deficit.

When an osteofibrous tunnel becomes thinner or its content increases, the chronic conflict of tendons against its walls may cause a stenosing tenosynovitis. This condition leads to pain and functional impairment and progresses to blockage or triggering of the affected tendon. De Quervain disease and trigger finger are the most frequently occurring stenosing tenosynovites that can be demonstrated with US. In both conditions the involved tendons are swollen with textural disarrangement and focal or diffuse thickening of the synovial sheath [58, 59, 60]. Simple synovial effusion is observed in acute cases, whereas chronic cases are associated with thickening of the retinaculum, which usually represents indication to operative

management. Dynamic examination with passive assisted movements may demonstrate the entrapment of the synovial sheath at the entrance of the narrowed tunnel.

Entrapment neuropathies typically occur within osteofibrous tunnels. The osteofibrous tunnels that are best suited for a US examination are the carpal tunnel for the median nerve and the cubital and Guyon tunnels for the ulnar nerve in the upper limb; the fibular neck for the common peroneal nerve, the tarsal tunnel for the tibial nerve, and the intermetatarsal spaces for the interdigital nerves in the lower limb [14]. Whatever the tunnel involved, the main US signs of nerve entrapment include changes in both nerve shape and echotexture, as a probable result of either intraneuronal edema and venous congestion or fibrosis, and increased depiction of intra- and perineural flow signals at color Doppler imaging as an expression of inflammatory hyperemia [14]. The nerve shape changes consist of abrupt flattening of the nerve at the compression site and fusiform hypoechoic swelling at a more proximal level (Fig. 6) [61, 62, 63, 64]. These signs are more clearly appreciated in chronic, long-term disease. To reduce some bias related to subjectivity, quantitative analysis has also been applied at carpal and cubital tunnel syndromes by means of calculation of a series of indexes, such as the nerve cross-sectional area, although chronicity of the disease, and severity of symptoms may have an influence on these parameters [61, 62, 65, 66, 68]; however, the area of median nerve at carpal tunnel has proved to correlate well

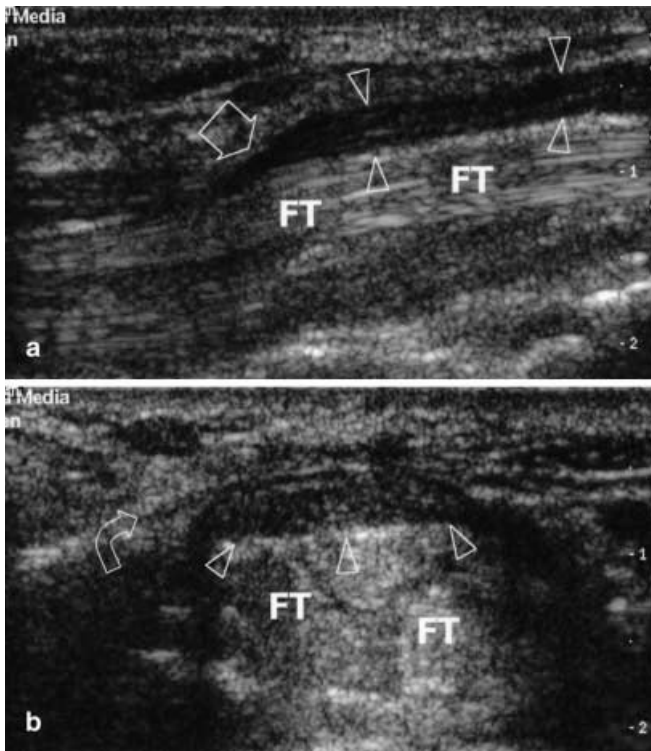


**Fig. 6a, b** Carpal tunnel syndrome. **a** Longitudinal 12- to 5-MHz US scan shows abrupt flattening (*straight arrow*) of the median nerve in the carpal tunnel and swelling of the nerve proximal to the compression point (*arrowheads*). FT flexor tendons. **b** Transverse US image at the proximal tunnel. The median nerve (*arrowheads*) is markedly enlarged and the shape of the overlying flexor retinaculum (*curved arrow*) is convex

with the severity of electromyographic features [67]. Other accessory findings, such as bowing or thickening of the retinaculum and reduced mobility of the nerve within the tunnel have also been described, and especially at the carpal tunnel level [61, 62, 65, 68]. Ultrasound has also proved to be an accurate means in detecting a variety of abnormalities for nerve entrapment, including either congenital anomalies (i.e., accessory muscles, accessory vessels) or acquired disease, which in turn lead to either an increased content (i.e., tenosynovitis of adjacent tendons, ganglion cysts, soft tissue masses, and neoplasms) or a decreased size (i.e., anomalous bone within the tunnel, fractures, osteophytes) of the tunnel [14, 63, 69, 70, 71, 72, 73]. In this setting, US may enhance the diagnosis and the surgical result by providing information on the nature of constricting findings, especially in cases with confusing clinical pictures or ambiguous functional studies. In addition, if the patient's symptoms are not typical, US can be an effective means in exploring the entire course of the nerve in order to rule out other, more proximal, levels of compression.

Local entrapment below the distal edge of the intermetatarsal ligament, ischemia, and compression of the

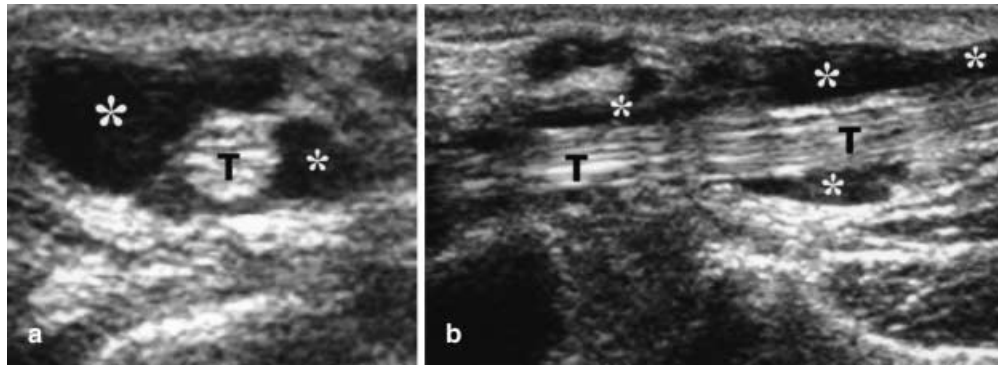
nerve by an inflamed intermetatarsal bursa are possible pathogeneses of Morton neuromas. These lesions most frequently occur in the second or third interspace, and are located at the level of or slightly proximal to the metatarsal heads. Sonographically, they appear as fusiform hypoechoic masses elongated along the major axis of metatarsals [74, 75, 76]. In this field, US has a reported sensitivity of 95–100%, with specificity of 83% and accuracy of 95% [74, 75, 77]. Small lesions can be difficult to evaluate with US [78], but identification of the plantar digital nerve in continuity with the mass improves diagnostic confidence [76].

### Inflammatory and infectious diseases

The term “tendinitis” reflects an inflammatory response that occurs, at any extent, in tendons. It has to be considered that this term is widely used inopportunely. In fact, in several pathologic conditions, tendinitis is a misnomer with respect to the histopathologic classification, especially when degenerative (i.e., proliferation of fibroblasts and vascular connective tissue) and not inflammatory changes are found. In such cases the entire process may be referred to more accurately as “tendinosis”. Nevertheless, some pathologic conditions in tendons are inflammatory in nature, and distinction from simple tendinosis is important because clinical management may differ. Although both conditions may be treated with conservative measures (i.e., rest and anti-inflammatory drugs), inflammatory lesions that fail to regress may require more aggressive therapy with corticosteroids or even surgical procedures.

The spectrum of US findings depends on the type of tendon involved, as well as on the associated changes occurring in the tendon envelopes and paratendinous synovial bursae. In tendons with paratenon, the inflammatory process results mainly in “peritendinitis,” which appears as a patchy thickening of the paratenon, irregularities of tendon margins, fluid collection, and adhesions among paratenon and peritendinous tissues [24]. In synovial sheath tendons, inflammation is mostly secondary to repetitive microtrauma. Acute serous tenosynovitis is diagnosed by identifying increased amount of fluid within the tendon's sheath, often associated with peritendinous hyperemia, whereas in subacute or chronic tenosynovitis the effusion is often associated with sheath thickening (Fig. 7) [79, 80, 81]. Careful scanning technique is needed to demonstrate small but significant synovial effusions which, for instance, can be easily unrecognized if excessive pressure by the scanhead causes collapse of the sheath. Depending on its cellular content, the fluid in the synovial sheath may be anechoic or may contain subtle echoes in suspension [82]. In infective tenosynovitis, the effusion tends to be more echogenic and the overlying subcutaneous tissue may appear thickened and hyperechoic due to cellulitis [83, 84, 85]; however, it

**Fig. 7a, b** Acute tenosynovitis. **a** Transverse and **b** longitudinal 10- to 5-MHz US scans at wrist demonstrate enlargement of the sheath of flexor carpi radialis tendon (*T*) by hypoechoic fluid (*asterisk*). In **a**, the presence of synovial effusion allows depiction of the anatomy of the synovial sheath and mesotendon



must be emphasized that these characteristics are too subtle to allow a definitive diagnosis based on US findings alone. Needle aspiration of fluid, possibly obtained under US guidance, is necessary to confirm the infectious nature of tenosynovitis [84]. As an exception to this rule, the diagnosis may be straightforward on US findings when a foreign body is recognized within the synovial sheath [86]. In tuberculous tenosynovitis, the tendon sheaths appear markedly thickened as a result of granulomatous changes [87]. In rheumatoid arthritis, hypoechoic villous projections of the synovium (pannus) can develop inside the effusion up to fill the synovial space (Fig. 8). Many tendons are contemporary involved, and especially the extensor carpi ulnaris along with other flexor and extensor digitorum tendons at wrist and the posterior tibial tendon [88, 89, 90, 91, 92, 93]. The biochemical damage due to the lytic action of the pannus increases the incidence of tendon ruptures, and US can be used to differentiate the functional impairment due to joint disease from tendons tears. Ultrasound transducer compression can be helpful in differentiate complex effusion from synovial thickening because fluid may be squeezed away compared with the noncompressible synovium [88]. Similarly, color Doppler imaging seems promising in distinguishing the hypoechoic pannus from the effusion based on the presence or absence of flow signals, as well as in differentiating the highly vascular, active pannus from the hypovascular fibrous pannus [94]. Future possibilities include follow-up of disease progression and quantification of response to therapy.

A wide spectrum of nerve abnormalities at US due to inflammatory and degenerative changes, acute reactional states, and entrapment syndromes have been reported in patients with Hansen disease, a chronic infectious disease caused by *Mycobacterium leprae* which, in its many and various clinical forms, primarily involves the skin and nerves [95, 96]. In lepromatous patients, the nerve hypertrophy is considered to be a main feature. By measuring the nerve cross-sectional area with US, it was pointed out that the increased nerve size correlates with acute reactional states [96]. During these reactions, endoneural color flow signals as well as increased T2 sig-

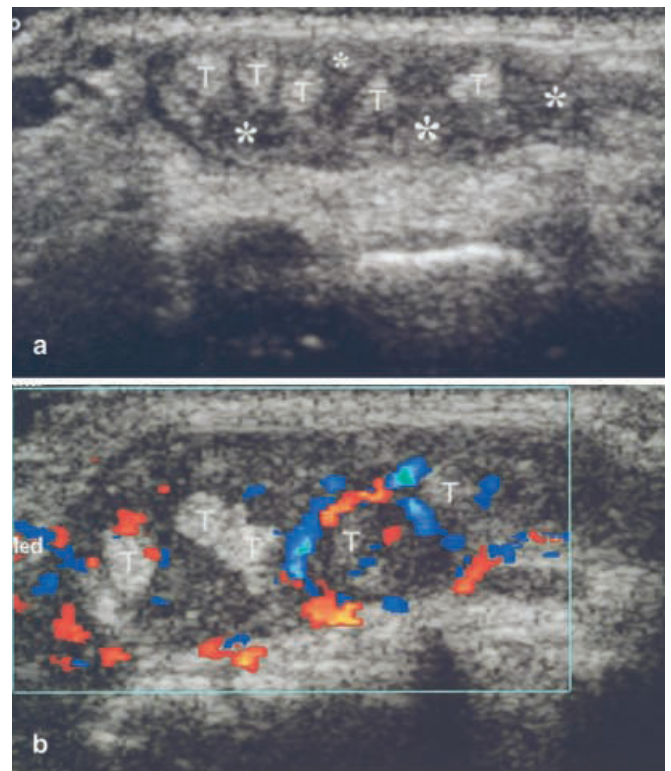


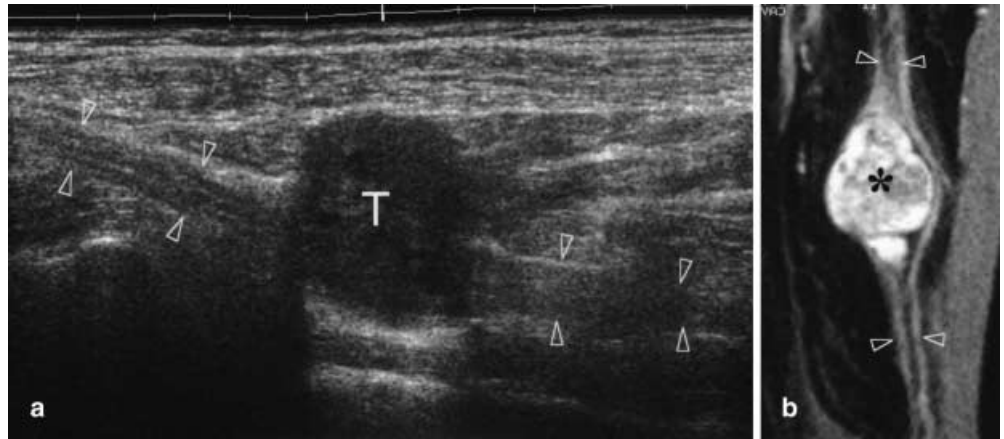
**Fig. 8a, b** Rheumatoid arthritis. **a** Transverse 12- to 5-MHz grayscale and **b** color Doppler US scan at the dorsum of wrist shows a hypertrophic synovial pannus (*asterisks*) in the fourth compartment of extensor digitorum tendons (*T*). The pannus appears echogenic, noncompressible, and hypervascular at color Doppler imaging; therefore, it can easily be differentiated from an effusion

nal and gadolinium enhancement indicate rapid progression of nerve damage and a poor prognosis unless antireaction treatment is started [96].

#### Space-occupying lesions

Primary tumors arising from tendons are exceptional [69, 97]. On the contrary, nonneoplastic expansible le-

**Fig. 9a, b** Schwannoma of the tibial nerve at the posterior leg. **a** Longitudinal 12- to 5-MHz US scan with **b** fat-saturated T2-weighted turbo SE MR imaging correlation depicts the tumor (*T*) as an oval homogeneous hypoechoic mass in continuity with the tibial nerve (arrowheads)



sions, such as ganglia and localized giant cell tumor of tendon sheath, are much more common. Although most of these lesions present as a focal painless soft tissue swelling in the extremities, their mass effect may lead to compression of adjacent structures or transient arrest of motion, especially if the mass develops in proximity to retinacula or within a tunnel. Ganglion cysts may be encountered adjacent to the sheath of a tendon. These lesions are histologically composed of a fibrous capsule filled with mucoid viscid fluid and typically involve tendons at the dorsum of the hand and foot [98]. At US they appear as rounded or lobulated homogeneous anechoic cysts with acoustic enhancement, although internal low-level echoes may be encountered in longstanding or inflamed lesions. Occasionally, ganglia expands within the tendon substance, weaken the tendon structure, and predispose it to rupture. In these instances dynamic examination induces changes in position and shape of the ganglion and can help to define its intratendinous nature [98]. Ultrasound-guided needle aspiration of the fluid content of ganglion cysts has been reported, but this procedure seems to predispose to recurrences [99]. The giant cell tumor of tendon sheath preferentially usually presents as a painless soft tissue swelling affecting the volar aspect of digits with lateral and circumferential extension. Ultrasound shows a nonspecific solid hypoechoic mass adjacent to a normally appearing tendon [86]. Cortical bone erosions of the phalanges, secondary to pressure from the overlying lesion, and displacement of the digital arteries, can also be appreciated. After surgery, US may be helpful for screening recurrences related to local invasivity of this lesion.

Nerve tumors are divided in two major benign categories, schwannoma and neurofibroma, and a malignant form, malignant peripheral nerve sheath tumor. Each category can be associated with type-1 (von Recklinghausen) neurofibromatosis. Sonographically, nerve tumors usually present a fusiform shape oriented longitudinally in the nerve axis, revealing tapered ends that are in continuity with the nerve of origin (Fig. 9). Detection of a soft tis-

sue mass associated with neurologic symptoms and muscle atrophy in a typical nerve distribution are the main clinical features. Most lesions appear as hypoechoic masses and have well-defined margins [1, 100]. Associated findings are the “split fat” and the “target” sign, which are similar to those already described at MR imaging [101, 102]. The US findings of schwannomas are similar to those in neurofibromas and, in many cases, these tumor histotypes cannot be distinguished. Neurofibromas develop as centrally located masses, whereas schwannomas tend to grow eccentrically to the nerve, thus requiring a careful scanning technique because the nerve ends may be distorted and stretched over the tumor. Heterogeneous appearance, hypervascular pattern, and intratumor cystic changes are most common in schwannomas [103]. In type-1 (von Recklinghausen) neurofibromatosis, a genetically transmitted disorder, innumerable plexiform neurofibromas may thicken long segments of the involved nerves, extending in the secondary branches and resulting in the so-called bag of worms appearance [104]. The diffuse form of neurofibromatosis presents with ill-defined masses within the subcutaneous tissue. Similar to other imaging modalities, US is not able to give a confident differentiation between benign and malignant neurogenic masses. The main signs of malignancy are: large tumor size (>5 cm); ill-defined margins suggesting edema and infiltration of adjacent tissues; calcifications; and heterogeneous structure with central necrosis [102]; however, it must be noted that benign lesions can also share these features.

Nerve sheath ganglia most frequently involve the large nerves about the knee, and especially the peroneal nerve at the level of fibular head. They may be extension of ganglia related to the proximal tibiofibular joint that typically infold in the space between the epineurium and the nerve fascicles or may arise primarily in the nerve sheath. Patients present with a palpable mass and neurologic symptoms resulting from nerve compression. Sonographically, these ganglia appear as spindle-shaped cysts in the nerve and may contain septations [104].

## References

- Fornage BD (1988) Peripheral nerves of the extremities: imaging with US. *Radiology* 167:179–182
- Jacobson JA, van Holsbeeck MT (1998) Musculoskeletal ultrasonography. *Orthop Clin North Am* 29:135–167
- Martinoli C, Bianchi S, Derchi LE (1999) Tendon and nerve sonography. *Radiol Clin North Am* 37:691–711
- Martinoli C, Bianchi S, Derchi LE (2000) Ultrasonography of peripheral nerves. *Semin Ultrasound CT MR* 21:205–213
- Erickson SJ (1997) High-resolution imaging of the musculoskeletal system. *Radiology* 205:593–618
- Fornage BD, Rifkin MD (1988) Ultrasound examination of tendons. *Radiol Clin North Am* 6:87–107
- Martinoli C, Derchi LE, Pastorino C, Bertolotto M, Silvestri E (1993) Analysis of echotexture of tendons with US. *Radiology* 186:839–843
- Graif M, Seton A, Nerubali J et al. (1991) Sciatic nerve: sonographic evaluation and anatomic-pathologic considerations. *Radiology* 18:405–408
- Silvestri E, Martinoli C, Derchi LE et al. (1995) Echotexture of peripheral nerves: correlation between US and histologic findings and criteria to differentiate tendons. *Radiology* 197:291–296
- Bianchi S, Zwass A, Abdelwahab IF, Banderali A (1994) Diagnosis of tears of the quadriceps tendon of the knee: value of sonography. *Am J Roentgenol* 162:1137–1140
- Bertolotto M, Perrone R, Martinoli C et al. (1995) High-resolution ultrasound anatomy of normal Achilles tendon. *Br J Radiol* 68:986–991
- Sheppard DG, Iyer RB, Fenstermacher MJ (1998) Brachial plexus: demonstration at US. *Radiology* 208:402–406
- Yang WT, Chui PT, Metreweli C (1998) Anatomy of the normal brachial plexus revealed by sonography and the role of sonographic guidance in anesthesia of the brachial plexus. *Am J Roentgenol* 171:1631–1636
- Martinoli C, Bianchi S, Gandolfo N, Valle M, Simonetti S, Derchi LE (2000) US of nerve entrapments in osteofibrous tunnels of the upper and lower limbs. *Radiographics* 20:199–217
- Martinoli C, Bianchi S, Nebiolo M, Derchi LE, Garcia F (2000) Sonographic evaluation of digital annular pulley tears. *Skeletal Radiol* 29:387–391
- Fornage BD (1987) The hypoechoic normal tendon: a pitfall. *J Ultrasound Med* 6:19–22
- Giovagnorio F, Martinoli C (2001) Sonography of the cervical vagus nerve: normal appearance and abnormal findings. *Am J Roentgenol* 176:745–749
- Kainberger F, Mittermaier F, Seidl G, Parth E, Weinstabl R (1997) Imaging of tendons: adaptation, degeneration, rupture. *Eur J Radiol* 25:209–222
- Weinberg EP, Adams MJ, Hollenberg GM (1998) Color Doppler sonography of patellar tendinosis. *Am J Roentgenol* 171:743–744
- Khan KM, Bonar F, Desmond PM et al. (1996) Patellar tendinosis (jumper's knee): findings at histopathologic examination, US and MR imaging. *Radiology* 200:821–827
- Movin T, Gad A, Reinholt FP, Rolf C (1997) Tendon pathology in long-standing achillobodynia. Biopsy findings in 40 patients. *Acta Orthop Scand* 68:170–175
- Maffulli N, Regine R, Carrillo F et al. (1990) Tennis elbow: an ultrasonographic study in tennis players. *Br J Sports Med* 24:151–155
- Khan KM, Cook JL, Visentini PJ et al. (1997) Patellar tendon ultrasonography and jumper's knee in female basketball players: a longitudinal study. *Clin J Sport Med* 7:199–206
- Gibbon WW, Cooper JR, Radcliffe GS (2000) Distribution of sonographically detected tendon abnormalities in patients with a clinical diagnosis of chronic Achilles tendinosis. *J Clin Ultrasound* 28:61–66
- Connell D, Burke F, Coombes P et al. (2001) Sonographic examination of lateral epicondylitis. *Am J Roentgenol* 176:1763–1777
- Kainberger F, Seidl G, Traindl O et al. (1993) Ultrasonography of the Achilles tendon in hypercholesterolemia. *Acta Radiol* 34:408–412
- Bude RO, Adler RS, Bassett DR, Ikeda DM, Rubin JM (1993) Heterozygous familial hypercholesterolemia: detection of xanthomas in the Achilles tendon with US. *Radiology* 188:567–571
- Bude RO, Nesbitt SD, Adler RS, Rubenfire M (1998) Sonographic detection of xanthomas in normal-sized Achilles tendons of individuals with heterozygous familial hypercholesterolemia. *Am J Roentgenol* 170:621–625
- Bureau NJ, Roederer G (1998) Sonography of Achilles tendon xanthomas in patients with heterozygous familial hypercholesterolemia. *Am J Roentgenol* 171:745–749
- Yu JS, Witte D, Resnick D et al. (1994) Ossification of the Achilles tendon: imaging abnormalities in 12 patients. *Skeletal Radiol* 23:127–131
- Olivieri I, Barozzi L, Padula A (1998) Enthesiopathy: clinical manifestations, imaging and treatment. *Baillieres Clin Rheumatol* 12:665–681
- Farin PU, Jaroma H (1995) Sonographic findings of rotator cuff calcifications. *J Ultrasound Med* 14:7–14
- De Flaviis L, Nessi R, Scaglione P et al. (1989) Ultrasonic diagnosis of Osgood-Schlatter and Sinding-Larsen-Johansson diseases of the knee. *Skeletal Radiol* 18:193–197
- Lanning P, Heikkinen E (1991) Ultrasonic features of the Osgood-Schlatter lesion. *J Pediatr Orthop* 11:538–540
- Kalebo P, Goksoer LA, Sward L, Peterson L (1990) Soft-tissue radiography, computed tomography, and ultrasonography of partial Achilles tendon ruptures. *Acta Radiol* 31:565–570
- Kalebo P, Allenmark C, Peterson L, Sward L (1992) Diagnostic value of ultrasonography in partial ruptures of the Achilles tendon. *Am J Sports Med* 20:378–381
- O'Reilly MAR, Massouth H (1993) Pictorial review: the sonographic diagnosis of pathology in the Achilles tendon. *Clin Radiol* 48:202–206
- Miller TT, Adler RS (2000) Sonography of tears of the distal biceps tendon. *Am J Roentgenol* 175:1081–1086
- Waitches GM, Rockett M, Brage M et al. (1998) Ultrasonographic-surgical correlation of ankle tendon tears. *J Ultrasound Med* 17:249–256
- Diaz GC, van Holsbeeck MT, Jacobson JA (1998) Longitudinal split of the peroneus longus and peroneus brevis tendons with disruption of the superior peroneal retinaculum. *J Ultrasound Med* 17:525–529
- Kainberger FM, Engel A, Barton P et al. (1990) Injury of the Achilles tendon: diagnosis with sonography. *Am J Roentgenol* 155:1031–1036
- Bianchi S, Zwass A, Abdelwahab IF, Zoccola C (1994) Evaluation of tibial anterior tendon rupture by ultrasonography. *J Clin Ultrasound* 22:564–566
- Farin PU (1996) Sonography of the biceps tendon of the shoulder: normal and pathologic findings. *J Clin Ultrasound* 24:309–316
- Chen YJ, Liang SC (1997) Diagnostic efficacy of ultrasonography in stage I posterior tibial tendon dysfunction: sonographic-surgical correlation. *J Ultrasound Med* 16:417–423

45. Lee DH, Robbin ML, Galliot R, Graveman VA (2000) Ultrasound evaluation of flexor tendon lacerations. *J Hand Surg [Am]* 25:236–241
46. Bodner G, Buchberger W, Schocke M et al. (2001) Radial nerve palsy associated with humeral shaft fracture: evaluation with US: initial experience. *Radiology* 219:811–816
47. Bodner G, Huber B, Schwabegger A, Lutz M, Waldenberger P (1999) Sonographic detection of radial nerve entrapment within a humerus fracture. *J Ultrasound Med* 20:131–136
48. Simonetti S, Bianchi S, Martinoli C (1999) Neurophysiological and ultrasound findings in sural nerve lesions following stripping of the small saphenous vein. *Muscle Nerve* 22:1724–1726
49. Farin PU, Jaroma H, Harju A et al. (1995) Medial displacement of the biceps brachii tendon: evaluation with dynamic sonography during maximal external shoulder rotation. *Radiology* 195:845–848
50. Ptaszniak R, Hennessy O (1995) Abnormalities of the biceps tendon of the shoulder: sonographic findings. *Am J Roentgenol* 164:409–414
51. Prato N, Derchi LE, Martinoli C (1996) Sonographic diagnosis of biceps tendon dislocation. *Clin Radiol* 51:737–739
52. Fessel DP, Vanderschueren GM, Jacobson JA et al. (1998) US of the ankle: technique, anatomy, and diagnosis of pathologic conditions. *Radiographics* 18:325–340
53. Magnano GM, Occhi M, Stadio M di, Tomà P, Derchi LE (1998) High-resolution US of non-traumatic recurrent dislocation of the peroneal tendons: a case report. *Pediatr Radiol* 28:476–477
54. Klauser A, Bodner G, Frauscher F, Gabl M, Zur Nedden D (1999) Finger injuries in extreme rock climbers. Assessment of high-resolution ultrasonography. *Am J Sports Med* 27:733–737
55. Bodner G, Rudisch A, Gabl M, Judmaier W, Springer P, Klauser A (1999) Diagnosis of digital flexor tendon annular pulley disruption: comparison of high frequency ultrasound and MRI. *Ultraschall Med* 20:131–136
56. Hauger O, Chung CB, Lektrakul N et al. (2000) Pulley system in the fingers: normal anatomy and simulated lesions in cadavers at MR imaging, CT and US with and without contrast material distention of the tendon sheath. *Radiology* 217:201–212
57. Okamoto M, Abe M, Shirai H, Ueda N (2000) Morphology and dynamics of the ulnar nerve in the cubital tunnel. Observation by ultrasonography. *J Hand Surg [Br]* 25:85–89
58. Serafini G, Derchi LE, Quadri P et al. (1996) High resolution sonography of the flexor tendons in trigger fingers. *J Ultrasound Med* 15:213–219
59. Giovagnorio F, Andreoli C, De Cicco ML (1997) Ultrasonographic evaluation of de Quervain's disease. *J Ultrasound Med* 16:685–689
60. Nagaoka M, Matsuzaki H, Suzuki T (2000) Ultrasonographic examination of de Quervain's disease. *J Orthop Sci* 5:96–99
61. Buchberger W, Schon G, Strasser K et al. (1991) High-resolution ultrasonography of the carpal tunnel. *J Ultrasound Med* 10:531–537
62. Buchberger W, Judmaier W, Birbamer G et al. (1992) Carpal tunnel syndrome: diagnosis with high-resolution sonography. *Am J Roentgenol* 159:793–798
63. Chen P, Maklad N, Redwine M et al. (1997) Dynamic high-resolution sonography of the carpal tunnel. *Am J Roentgenol* 168:533–537
64. Keberle M, Jennett M, Kenn W et al. (2000) Technical advances in ultrasound and MR imaging of carpal tunnel syndrome. *Eur Radiol* 10:1043–1050
65. Duncan I, Sullivan P, Lomas F (1999) Sonography in the diagnosis of carpal tunnel syndrome. *Am J Roentgenol* 173:681–683
66. Chiou HJ, Chou YH, Cheng SP et al. (1998) Cubital tunnel syndrome: diagnosis by high-resolution ultrasonography. *J Ultrasound Med* 17:643–648
67. Lee D, van Holsbeeck MT, Janevski PK et al. (1999) Diagnosis of carpal tunnel syndrome. Ultrasound versus electromyography. *Radiol Clin North Am* 37:859–872
68. Nakamichi K, Tachibana S (1995) Restricted motion of the median nerve in carpal tunnel syndrome. *J Hand Surg [Br]* 20:460–464
69. Bertolotto M, Rosenberg I, Parodi RC et al. (1996) Case report: fibroma of tendon sheath in the distal forearm with associated median nerve neuropathy: US, CT and MR appearance. *Clin Radiol* 51:370–372
70. Kato H, Ogino T, Nanbu T et al. (1991) Compression neuropathy of the motor branch of the median nerve caused by palmar ganglion. *J Hand Surg [Am]* 16:751–752
71. Van Vugt RM, van Dalen A, Bijlsma JW (1998) The current role of high-resolution ultrasonography of the hand and wrist in rheumatic diseases. *Clin Exp Rheumatol* 16:454–458
72. Puig S, Turkof E, Sedivy R et al. (1999) Sonographic diagnosis of recurrent ulnar nerve compression by ganglion cysts. *J Ultrasound Med* 18:433–436
73. Nakamichi K, Tachibana S, Kitajima I (2000) Ultrasonography in the diagnosis of ulnar tunnel syndrome caused by an occult ganglion. *J Hand Surg [Br]* 25:503–504
74. Redd RA, Peters VJ, Emery SF et al. (1989) Morton neuroma: sonographic evaluation. *Radiology* 171:415–417
75. Shapiro PP, Shapiro SL (1995) Sonographic evaluation of interdigital neuromas. *Foot Ankle Int* 16:604–606
76. Quinn TJ, Jacobson JA, Craig JG, van Holsbeeck MT (2000) Sonography of Morton's neuromas. *Am J Roentgenol* 174:1723–1728
77. Read JW, Noakes JB, Kerr D et al. (1999) Morton's metatarsalgia: sonographic findings and correlated histopathology. *Foot Ankle Int* 20:153–161
78. Sobiesk GA, Wertheimer SJ, Schulz R et al. (1997) Sonographic evaluation of interdigital neuromas. *J Foot Ankle Surg* 36:364–366
79. Gooding GAW (1988) Tenosynovitis of the wrist. A sonographic demonstration. *J Ultrasound Med* 7:225–226
80. Stephenson CA (1990) Sonographic diagnosis of tenosynovitis of the posterior tibial tendon. *J Clin Ultrasound* 18:114–116
81. Bredahl WH, Stafford Johnson DB, Newman JS, Adler RS (1998) Power Doppler sonography in tenosynovitis: significance of the peritendinous hypoechoic rim. *J Ultrasound Med* 17:103–107
82. Bianchi S, Martinoli C, Abdelwahab IF (1999) High-frequency ultrasound examination of the wrist and hand. *Skeletal Radiol* 28:121–129
83. Jeffrey RB Jr, Laing FC, Schechter WP, Markison RE, Barton RM (1987) Acute suppurative tenosynovitis of the hand: diagnosis with US. *Radiology* 162:741–742
84. Schechter WP, Markison RE, Jeffrey RE Jr, Barton RM, Laing FC (1989) Use of sonography in the early detection of suppurative flexor tenosynovitis. *J Hand Surg* 14:307–310
85. Bureau NJ, Chhem RK, Cardinal E (1999) Musculoskeletal infections: US manifestations. *Radiographics* 19:1585–1592
86. Howden MD (1994) Foreign bodies within finger tendon sheaths demonstrated by ultrasound: two cases. *Clin Radiol* 49:419–420
87. Riehl J, Schmitt H, Bergmann D, Sieberth HG (1997) Tuberculous tenosynovitis of the hand: evaluation with B-mode ultrasonography. *J Ultrasound Med* 16:369–372
88. De Flaviis L, Scaglione P, Nessi R (1988) Ultrasonography of the hand in rheumatoid arthritis. *Acta Radiol* 29:457–460

- 
89. Fornage BD, Rifkin MD (1988) Ultrasound examination of the hand and foot. *Radiol Clin North Am* 26:109–129
  90. Fornage BD (1989) Soft-tissue changes in the hand in rheumatoid arthritis: evaluation with US. *Radiology* 173:735–737
  91. Grassi W, Tittarelli E, Blasetti P, Pirani O, Cervini C (1995) Finger tendon involvement in rheumatoid arthritis. Evaluation with high-frequency sonography. *Arthritis Rheum* 38:786–794
  92. Coakley FV, Samanta AK, Finlay DB (1994) Ultrasonography of the tibial posterior tendon of the knee: value of sonography. *Br J Rheumatol* 33:273–277
  93. Kotob H, Kamel M (1999) Identification and prevalence of rheumatoid nodules in the finger tendons using high frequency ultrasonography. *J Rheumatol* 26:1264–1268
  94. Newman JS, Laing TJ, McCarthy CJ et al. (1996) Power Doppler sonography of synovitis: assessment of therapeutic response – preliminary observations. *Radiology* 198:582–584
  95. Fornage BD, Nerot C (1987) Sonographic diagnosis of tuberculoid leprosy. *J Ultrasound Med* 6:105–107
  96. Martinoli C, Derchi LE, Bertolotto M et al. (2000) US and MR imaging of peripheral nerves in leprosy. *Skeletal Radiol* 29:142–150
  97. Silvestri E, Bertolotto M, Perrone R (1994) Case report: US detection of tendinous metastasis from malignant melanoma. *Clin Radiol* 49:288–289
  98. Bianchi S, Abdelwahab IF, Zwass A et al. (1993) Sonographic findings in examination of digital ganglia: retrospective study. *Clin Radiol* 48:45–47
  99. Kato H, Minami A, Hirachi K et al. (1997) Treatment of flexor tendon sheath ganglions using ultrasound imaging. *J Hand Surg [Am]* 22:1027–1033
  100. Beggs I (1999) Sonographic appearances of nerve tumors. *J Clin Ultrasound* 27:363–368
  101. Lin J, Jacobson JA, Hayes CW (1999) Sonographic target sign in neurofibromas. *J Ultrasound Med* 18:513–517
  102. Lin J, Martel W (2001) Cross-sectional imaging of peripheral nerve sheath tumors: characteristic signs on CT, MR imaging, and sonography. *Am J Roentgenol* 176:75–82
  103. King AD, Ahuja AT, King W et al. (1997) Sonography of peripheral nerve tumors of the neck. *Am J Roentgenol* 169:1695–1698
  104. Murphey MD, Smith WS, Smith SE et al. (1999) Imaging of musculoskeletal neurogenic tumors: radiologic–pathologic correlation. *Radiographics* 19:1253–1280